

## Rad18 Regulates DNA Polymerase $\kappa$ and Is Required for Recovery from S-Phase Checkpoint-Mediated Arrest

Xiaohui Bi,<sup>1†</sup> Laura R. Barkley,<sup>1†</sup> Damien M. Slater,<sup>1</sup> Satoshi Tateishi,<sup>2</sup> Masaru Yamaizumi,<sup>2</sup> Haruo Ohmori,<sup>3</sup> and Cyrus Vaziri<sup>1\*</sup>

Department of Genetics and Genomics, Boston University School of Medicine, 80 E. Concord St., Boston, Massachusetts 02118<sup>1</sup>; Institute of Molecular Embryology and Genetics, Kumamoto University, Honjo 2-2-1, Kumamoto 860-0811, Japan<sup>2</sup>; and Institute for Virus Research, Kyoto University, 53 Shogoin-Kawaracho, Sakyo-ku, Kyoto 606-8507, Japan<sup>3</sup>

Received 15 November 2005/Returned for modification 21 December 2005/Accepted 14 February 2006

**We have investigated mechanisms that recruit the translesion synthesis (TLS) DNA polymerase Polk to stalled replication forks. The DNA polymerase processivity factor PCNA is monoubiquitinated and interacts with Polk in cells treated with the bulky adduct-forming genotoxin benzo[*a*]pyrene dihydrodiol epoxide (BPDE). A monoubiquitination-defective mutant form of PCNA fails to interact with Polk. Small interfering RNA-mediated downregulation of the E3 ligase Rad18 inhibits BPDE-induced PCNA ubiquitination and association between PCNA and Polk. Conversely, overexpressed Rad18 induces PCNA ubiquitination and association between PCNA and Polk in a DNA damage-independent manner. Therefore, association of Polk with PCNA is regulated by Rad18-mediated PCNA ubiquitination. Cells from *Rad18*<sup>-/-</sup> transgenic mice show defective recovery from BPDE-induced S-phase checkpoints. In *Rad18*<sup>-/-</sup> cells, BPDE induces elevated and persistent activation of checkpoint kinases, indicating persistently stalled forks due to defective TLS. *Rad18*-deficient cells show reduced viability after BPDE challenge compared with wild-type cells (but survival after hydroxyurea or ionizing radiation treatment is unaffected by *Rad18* deficiency). Inhibition of RPA/ATR/Chk1-mediated S-phase checkpoint signaling partially inhibited BPDE-induced PCNA ubiquitination and prevented interactions between PCNA and Polk. Taken together, our results indicate that ATR/Chk1 signaling is required for Rad18-mediated PCNA monoubiquitination. Recruitment of Polk to ubiquitinated PCNA enables lesion bypass and eliminates stalled forks, thereby attenuating the S-phase checkpoint.**

Polycyclic aromatic hydrocarbons (PAHs) are abundant and ubiquitous environmental pollutants with well-documented mutagenic and carcinogenic properties (4). The biological effects of the PAH benzo[*a*]pyrene (B[*a*]P) have been studied extensively in vivo and in vitro. B[*a*]P and many related PAHs are subject to intracellular cytochrome P450-mediated metabolism (11). Cytochrome P450-dependent oxidation of B[*a*]P generates the reactive species and ultimate carcinogen B[*a*]P dihydrodiol epoxide (BPDE). BPDE can react covalently with exocyclic deoxyguanosine (majority, ~90%) and deoxyadenosine (minority, ~10%) residues in genomic DNA to generate bulky adducts (18). The DNA adducts resulting from covalently bound BPDE are believed to account for the mutagenic and carcinogenic properties of B[*a*]P (19). Potentially, error-prone repair or replication of BPDE-adducted DNA can result in mutations. Propagation of cells containing BPDE-induced mutations in oncogenes or tumor suppressor genes can contribute to multistep carcinogenesis.

Because of the potential threat to genomic stability posed by DNA adducts (as well as other forms of DNA damage), cells have evolved elaborate mechanisms to detect and repair damaged DNA. Cell cycle checkpoints are signal transduction pathways that respond to damaged DNA by inhibiting cell cycle progression (45). The cell cycle delays elicited by check-

point signaling enable integration of cell cycle progression with DNA repair. Consequently, checkpoints are important for preserving the integrity of the genome. Cells can acquire DNA damage throughout the cell cycle. Therefore, DNA damage-inducible checkpoint mechanisms exist that arrest cells in G<sub>1</sub>, S, and G<sub>2</sub>/M phases. Individuals with congenital defects in checkpoint genes (such as *ATM*, *ATR*, *p53*, and *CHEK2*) are prone to cancer, highlighting the importance of checkpoint signaling pathways as important tumor-suppressive mechanisms.

Cell cycle responses to DNA damage acquired during S phase are highly conserved in eukaryotes. During a normal S phase, DNA synthesis initiates at multiple loci (termed origins of replication) that are activated (a process known as firing) in a temporally ordered manner (17). When ongoing replication forks encounter DNA lesions, a signal is generated that prevents initiation of DNA synthesis from unfired origins. The inhibition of DNA synthesis due to delayed firing of late origins is termed the S-phase checkpoint (or the intra-S-phase checkpoint).

Bulky adducts such as those induced by BPDE and UV elicit an S-phase checkpoint pathway involving the proximal checkpoint components ATR (an ATM/RAD3-related protein kinase) and the heterotrimeric Rad9-Rad1-Hus1 (9-1-1) complex (20, 21, 44). ATR and 9-1-1 are recruited separately to damaged DNA (47, 48). Activation of ATR involves its recruitment to RPA-coated single-stranded DNA (ssDNA), which is generated by the uncoupling of replicative helicases from fork progression, via the ATR-interacting protein ATRIP (also termed Rad26) (47, 48). After recruitment to damaged DNA,

\* Corresponding author. Mailing address: Department of Genetics and Genomics, Boston University School of Medicine, 80 E. Concord St., Boston, MA 02118. Phone: (617) 638-4175. Fax: (617) 414-1646. E-mail: cvaziri@bu.edu.

† X.B. and L.R.B. contributed equally to this work.

the concerted actions of ATR and 9-1-1 activate the checkpoint kinase Chk1, which mediates the inhibition of late-firing origins in response to DNA damage. The mechanism by which Chk1 inhibits DNA synthesis at late origins might involve degradation of the Cdc25A protein phosphatase (38) and inhibition of the Dbf4-Cdc7 protein kinase complex (14, 15) which is required for initiation of DNA replication at individual origins throughout S phase. ATM, Nbs1, and Chk2 are dispensable for the BPDE-induced checkpoint pathway (44) and probably also for the UV-induced checkpoint. In addition to inhibiting initiation of late origins, S-phase checkpoint signaling is important for stabilizing stalled replication forks via an unknown mechanism(s) (16, 31, 40).

Replicative DNA polymerases are generally unable to carry out accurate or efficient DNA synthesis when they encounter bulky adducts or other lesions. However, specialized DNA polymerases can be used to replicate past lesions in a process termed translesion synthesis (TLS). Replicative bypass of DNA lesions is an inherently error-prone process due to the low fidelity of TLS polymerases. Thus, error-prone TLS is considered to be one of the causes of mutagenesis and carcinogenesis due to DNA lesions.

TLS DNA polymerases in mammalian cells include Pol $\kappa$ , Pol $\eta$ , Pol $\iota$ , Rev1 (the Y family polymerases), and Pol $\zeta$  (a B family polymerase comprising the catalytic Rev3 subunit and the noncatalytic Rev7 protein). Pol $\eta$  was the first mammalian TLS polymerase identified (25, 32). Pol $\eta$  is encoded by the *XPV* gene, which is defective in xeroderma pigmentosum variant patients. The role of mammalian Pol $\eta$  (and that of its *Saccharomyces cerevisiae* homologue encoded by the *Rad30* gene) in TLS has been studied extensively. Pol $\eta$  is unique among eukaryotic DNA polymerases in its ability to replicate templates containing *cis-syn* thymine-thymine dimers (the species generated by UV radiation).

Studies *in vitro* with yeast indicate that Pol $\eta$  promotes error-free DNA translesion synthesis in a manner which is stimulated by PCNA and regulated by the Rad6/Rad18 epistasis pathway (22, 39). Rad6 is an E2 ubiquitin (Ub)-conjugating enzyme (also termed UBC2) that forms a tight complex with the RING-containing E3 ligase Rad18. The Rad18-Rad6 complex binds ssDNA and has ssDNA-stimulated ATPase activity (2). Recent reports have demonstrated that in yeast and mammalian cells Rad18 is important for monoubiquitination of PCNA in response to DNA damage (22, 28, 39, 43). Moreover, Pol $\eta$  interacts preferentially with monoubiquitinated PCNA. It has also been shown that Rad18 and Pol $\eta$  interact via their C-terminal motifs and that this interaction is important for guiding Pol $\eta$  to PCNA (43). Therefore, according to current models, Rad18/Rad6-mediated monoubiquitination of PCNA constitutes a molecular switch that recruits Pol $\eta$  to stalled replication forks (41).

In contrast to Pol $\eta$ , which bypasses BPDE-adducted templates very poorly, Pol $\kappa$  is able to bypass benzo[a]pyrene-adducted guanine, efficiently inserting the correct C opposite the bulky lesion (36). Pol $\kappa$ -deficient mutant mouse embryonic stem (ES) cells are highly sensitive to B[a]P-induced mutagenesis and genotoxicity (35), further suggesting a role for Pol $\kappa$  in cellular responses to B[a]P-adducted DNA. BPDE, as well as hydroxyurea (HU) and UV irradiation, can elicit recruitment

of Pol $\kappa$  to nuclear foci (5, 6, 34), possibly suggesting a general role for Pol $\kappa$  in responses to genotoxins and replication stress.

Recently we showed that Pol $\kappa$  is specifically recruited to PCNA-containing foci in response to BPDE treatment concomitant with activation of the S-phase checkpoint (6). Furthermore, we showed that, in contrast to wild-type (WT) cells, Pol $\kappa^{-/-}$  mouse embryo fibroblasts (MEFs) arrested irreversibly in S phase after BPDE treatment. In BPDE-treated, Pol $\kappa$ -deficient cells, failure to recover from the S-phase checkpoint was associated with persistent activation of ATM, Chk1, and Chk2 kinases, and phosphorylation of the double-strand breakage (DSB) marker  $\gamma$ H2AX. Taken together, those results suggested that Pol $\kappa$ -mediated replicative bypass of BPDE adducts contributes to attenuation of DNA damage signaling and recovery from the S-phase checkpoint.

The specific mechanisms that recruit Pol $\kappa$  to the replication machinery in mammalian cells have not been identified. Because of the important role of Pol $\kappa$  in the BPDE-induced S-phase checkpoint, we have investigated the mechanisms that recruit Pol $\kappa$  to stalled replication forks and promote TLS. Experiments presented here demonstrate an important role for Rad18 in regulating PCNA monoubiquitination, Pol $\kappa$  recruitment, and S-phase checkpoint recovery. Importantly, we show that PCNA ubiquitination and associations between PCNA and Pol $\kappa$  are regulated by checkpoint signaling.

## MATERIALS AND METHODS

**Adenovirus construction and infection.** Adenovirus construction and infections were performed as described previously (20). cDNAs encoding hemagglutinin (HA)-Rad18 and HA-PCNA WT and PCNA K164A were subcloned into pAC-CMV to generate pAC-HA-Rad18 and pAC-PCNA WT and pAC-PCNA K164A, respectively. The resulting shuttle vectors were cotransfected into 293T cells with the pJM17 plasmid to generate recombinant adenovirus as described previously. AdGFP-Pol $\kappa$ , AdYFP-Pol $\eta$ , and AdChk1KR were described previously (6). H1299 cells were routinely infected with  $5 \times 10^9$  PFU/ml adenovirus. As controls for adenoviral infection, cells received AdCon (empty adenovirus vector) or AdGFP.

**Cell culture.** Human lung carcinoma H1299 cells, Rad18<sup>+/+</sup> and Rad18<sup>-/-</sup> MEFs, and TERT-immortalized xeroderma pigmentosum variant (*XPV*) CRL1162 fibroblasts were cultured in Dulbecco's modified Eagle's medium supplemented with 10% fetal bovine serum, streptomycin sulfate (100  $\mu$ g/ml), and penicillin (100 U/ml).

ET163 cells from ataxia-telangiectasia patients and a matched cell line designated YZ5, which is complemented with the ATM cDNA (46), were cultured in Dulbecco modified Eagle medium supplemented with 15% fetal bovine serum, streptomycin sulfate (100  $\mu$ g/ml), and penicillin (100 U/ml).

**Genotoxin treatments.** BPDE (National Cancer Institute carcinogen repository) was dissolved in anhydrous dimethyl sulfoxide and added directly to the growth medium as a 1,000 $\times$  stock to give a final concentration of 100 or 600 nM. For HU treatment, HU was dissolved in water and added directly to the growth medium as a 1,000 $\times$  stock to give a final concentration of 1  $\mu$ M. For UVC treatment, the growth medium was removed from the cells and replaced with phosphate-buffered saline (PBS). The plates were transferred to a UV cross-linker (Stratagene) and then irradiated. The UVC dose delivered to the cells was confirmed with a UV radiometer (UVP, Inc.). The cells were then refed with complete growth medium and returned to the incubator. For ionizing radiation (IR) treatment, cells were placed in PBS, irradiated with a cesium source, refed with complete growth medium, and then returned to the incubator. In some experiments, cells were incubated in medium containing 5 mM caffeine (Sigma) or 150 nM UCN-01 for 1 h before genotoxin treatment.

**RNA interference (RNAi).** Cells were plated into six-well culture dishes. At 24 h later, when cells were 50% confluent, the cultures were placed in P<sub>i</sub>-free medium (2 ml per well). For each transfection, 6.25  $\mu$ l of 20  $\mu$ M stocks of Cy3 (control) small interfering RNA (siRNA), siRPA, or siRAD18 or 10  $\mu$ l of siATR (Dharmacon smart pool) was diluted into 0.25 ml of Opti-MEM. After 5 min, the siRNA-Opti-MEM solution was mixed with 0.25 ml of Opti-MEM containing 5

$\mu$ l of Lipofectamine 2000. Twenty minutes later, the resulting mixture was added to culture medium. After incubation overnight, the transfection medium was removed and replaced with standard culture medium. All tubes, tips, and solutions used for RNAi experiments were certified RNase free.

**Clonogenic survival assays.** Cells were grown to 80% confluence, treated with genotoxins (as described above), and then split into replicate 10-cm plates at a density of 1,000 cells/plate. Cultures were given fresh medium every 3 days. After 1 week, colonies on the plates were fixed in methanol, stained with Giemsa, and counted.

**Analysis of PCNA ubiquitination with epitope-tagged Ub.** H1299 cells were plated into 10-cm culture dishes. When at 50% confluence, cells were infected with AdCon or AdRad18 for 24 h. Cells were then transfected with a hexahistidine- and Myc-tagged form of Ub (designated H<sub>6</sub>M-Ub). Eight micrograms of H<sub>6</sub>M-Ub was diluted into 1.5 ml of Opti-MEM. After 5 min, the DNA-Opti-MEM solution was mixed with 1.5 ml of Opti-MEM containing 20  $\mu$ l of Lipofectamine 2000. Twenty minutes later, the resulting mixture was added to 12 ml of culture medium. After incubation for 6 h, the transfection medium was removed and replaced with standard culture medium. At 24 h after transfection, cells were treated with 600 nM BPDE for 4 h prior to harvest. Cells were washed twice with PBS and then separated into soluble and insoluble fractions with cytoskeleton (CSK) buffer (23). The insoluble fraction was treated with 1,000 U/ml DNase (Roche 10776 785 001) for 30 min at room temperature and then clarified by centrifugation at  $10,000 \times g$  for 5 min. The supernatants (containing solubilized chromatin) were normalized for protein content. H<sub>6</sub>M-Ub-conjugated proteins were purified by overnight incubation at 4°C with 25  $\mu$ l of cobalt affinity resin (TALON Clontech 8901-2). The TALON resin was recovered by centrifugation and washed three times with CSK buffer and once with CSK buffer containing 50 mM imidazole. The washed TALON beads were resuspended in an equal volume of 2 $\times$  Laemmli buffer, boiled for 5 min, and resolved by sodium dodecyl sulfate-polyacrylamide gel electrophoresis (SDS-PAGE). Twenty percent of each input fraction was also analyzed by SDS-PAGE. After transfer to nitrocellulose, immunoblotting was performed with mouse monoclonal anti-PCNA (sc-56; Santa Cruz Biotechnology).

**DNA synthesis assays.** Cells were plated in 12-well culture dishes and grown to 60% confluence. Genotoxin treatments were performed as described above. To measure DNA synthesis at different time points after genotoxin treatment, replicate wells were given [<sup>3</sup>H]thymidine (1  $\mu$ Ci/ml; Perkin-Elmer Life Sciences) for 30 min. At the end of the labeling period, the [<sup>3</sup>H]thymidine-containing medium was aspirated and the monolayers were fixed by addition of 5% trichloroacetic acid. The fixed cells were washed three times with 5% trichloroacetic acid to remove unincorporated [<sup>3</sup>H]thymidine. The trichloroacetic acid-fixed cells were solubilized in 0.3 N NaOH. A 300- $\mu$ l aliquot of the NaOH-solubilized material was transferred to a scintillation vial and neutralized by addition of 100  $\mu$ l of glacial acetic acid. After addition of 5 ml of Ecocint scintillation fluid, incorporated [<sup>3</sup>H]thymidine was measured by scintillation counting.

For assays of DNA synthesis in transfected cells, 10-cm plates of *Rad18*<sup>-/-</sup> MEFs at ~60 to 80% confluence were placed in 5 ml of Opti-MEM. In a separate tube, 30  $\mu$ g of plasmid DNA and 50  $\mu$ l of Lipofectamine 2000 were added to 1.5 ml of Opti-MEM and mixed. The resulting mixture was incubated for 25 min at room temperature prior to addition to the cells. After 10 h, transfected cells were transferred to standard culture medium containing 10% FBS. Twelve hours later, the cells were split into 12-well culture dishes for DNA synthesis assays.

**Fluorescence microscopy.** Cells were plated in four-well chamber slides, grown to 30% confluence, and then infected with various adenovirus vectors. Twenty hours after infection, cells were treated with genotoxins for various times. In some experiments, yellow fluorescent protein (YFP)-Pol $\eta$  and HA-Polk were expressed by transient transfection of plasmid DNA. H1299 cells were seeded into six-well plates and cotransfected the following day with 2  $\mu$ g each of plasmids pcDNA3-Flag-HA-Polk and pAC.CMV-YFP-Pol $\eta$  (6) by using Lipofectamine 2000 (Invitrogen). Twenty-four hours after transfection, the cells were trypsinized, replated onto glass slides (Colorfrost Plus; Fisher), and grown for an additional 24 h. Cells were then treated with 600 nM BPDE for 6 h, solubilized with cold CSK buffer, and fixed with 1% paraformaldehyde.

To visualize green fluorescent protein (GFP)-Polk or YFP-Pol $\eta$  fluorescence, the cells were fixed with 4% paraformaldehyde for 10 min, washed with PBS, 4',6'-diamidino-2-phenylindole (DAPI) stained, and then mounted with Vectashield solution (Vector Laboratories). To visualize cellular proteins with antibodies, paraformaldehyde-fixed cells were permeabilized with 0.2% Triton X-100 for 5 min. After the slides were washed with PBS, cells were incubated overnight at 4°C with polyclonal HA antibody (Santa Cruz) diluted 1:100 in 1% bovine serum albumin (BSA)-PBS-Triton X-100 (PBST). The slides were washed three times with 1% BSA-PBST and then incubated for 1 h with Cy3-

conjugated donkey anti-mouse antibodies (Jackson ImmunoResearch) diluted 1:300 in 1% BSA-PBST. After being washed (three times with 1% BSA-PBST, 30 min per wash), the slides were DAPI stained and mounted with Vectashield solution (Vector Laboratories).

Slides were imaged and analyzed with a DeltaVision image restoration microscopy system (dv1301421; Applied Precision). In some experiments, cell populations were scored for constitutive and genotoxin-induced foci with a Nikon Eclipse E800 fluorescent microscope. In these studies, 500 cells were counted for each experimental condition.

**Immunoblotting.** Total cell lysates were prepared in lysis buffer containing 50 mM HEPES (pH 7.4), 0.1% Triton X-100, 150 mM NaCl, 1 mM EDTA, 50 mM NaF, 80 mM  $\beta$ -glycerophosphate, and 1 $\times$  protease inhibitor mixture (Roche Applied Science). In some experiments, whole nuclei were prepared with CSK buffer as described previously (6). Total cell extracts or nuclear protein samples were separated by SDS-PAGE, transferred to nitrocellulose, and analyzed by immunoblotting with the following antibodies: rabbit anti-Chk1 (FL-476; Santa Cruz Biotechnology), rabbit anti-Chk2 (H-300; Santa Cruz Biotechnology), mouse monoclonal anti-PCNA (catalog no. sc-56; Santa Cruz Biotechnology), rabbit anti-phospho-Chk1 Ser-345 (catalog number 2341; Cell Signaling), rabbit anti-phospho-Chk2 Thr-68 (catalog number 2661; Cell Signaling), polyclonal HA tag antibody (ab9110; abcam Inc.), and polyclonal PCNA antibody (FL-261, catalog no. sc-7907; Santa Cruz Biotechnology).

**Coimmunoprecipitation (co-IP) of PCNA and TLS DNA polymerases.** H1299 cells were plated in 10-cm culture dishes and infected with adenovirus as described above. Genotoxin treatments were performed at ~70% confluence. To isolate chromatin fractions for IP, cells were rinsed twice with PBS and then extracted with 5 ml of CSK buffer for 10 to 15 min. The CSK-extracted cells were rinsed once with PBS and then fixed with 1% formaldehyde in PBS (4.5 ml) for 10 min. Then, 0.5 ml of a 1 M glycine solution in PBS was added for 5 min to quench the cross-linking reaction. The cross-linked nuclei were rinsed with PBS and then lysed in 500  $\mu$ l of IP lysis buffer (freshly supplemented with protease and phosphatase inhibitors). Lysates were scraped from the plates and transferred into 1.5-ml Microfuge tubes. Samples were sonicated for two 8-s pulses at 30% of the maximum output. Pulses were separated by a 10-s interval on ice to prevent excessive heating. The sonicated samples were clarified by centrifugation at  $10,000 \times g$  for 5 min. Supernatants were removed and normalized for protein concentration (approximately 600  $\mu$ g of protein in 1 ml was used for each IP). PCNA was immunoprecipitated overnight at 4°C with 5  $\mu$ l of monoclonal PCNA antibody (Santa Cruz). A 25- $\mu$ l volume of protein A/G beads was added to each sample for 4 h. The beads were recovered by brief centrifugation and washed three times with 1 ml of IP lysis buffer (15 min per wash). The washed immune complexes were boiled in protein loading buffer for 25 min to reverse the cross-links prior to separation by SDS-PAGE.

In some experiments, cells were transfected with siRNA duplexes prior to analysis of PCNA-TLS polymerase associations. For these experiments, cultures were grown to 70 to 80% confluence and then transferred into 5 ml of P<sub>i</sub>-free medium. For siRNA transfections, 30  $\mu$ l of Cy3 control siRNA, siRPA, or siRAD18 stocks (all at 20  $\mu$ M) or 50  $\mu$ l of siATR stock solution (Dharmacon smart pool) was added to 1.25 ml of Opti-MEM. After 5 min, this was mixed with 1.25 ml of Opti-MEM containing 30  $\mu$ l of Lipofectamine 2000. Following a 25-min incubation at room temperature, the transfection mixture was added to the cells. After 24 h, when the cultures were fully confluent, the cells were split 1:2 into fresh 10-cm plates. These were infected with adenovirus vectors (AdGFP-Polk, AdChk1) for 24 h prior to genotoxin treatment. IPs were performed as described above.

**Co-IP of Rad18 and TLS polymerases.** H1299 cells growing in 10-cm plates were infected at 40 to 50% confluence with the various combinations of adenovirus for 36 h. Infected cells were treated with 600 nM BPDE for 6 h prior to harvest. Isolation of chromatin fractions for IP was performed essentially as described by Watanabe et al. (43). In brief, cells were washed twice with PBS and cross-linked with 9 ml of 1% formaldehyde for 10 min at room temperature. One milliliter of 1 M glycine was then added for 5 min at room temperature to quench the cross-linking reaction. Cells were washed twice in PBS and then fractionated into soluble and insoluble fractions with CSK buffer. The insoluble fraction was sonicated three times for 10 s at 30% of the maximum output and then clarified by centrifugation at  $10,000 \times g$  for 5 min. The supernatant (containing solubilized chromatin) and the soluble fraction from the initial cell lysis were normalized for protein content. GFP-Polk and YFP-Pol $\eta$  were immunoprecipitated overnight at 4°C with 3  $\mu$ l (6  $\mu$ g) of GFP antibody (Molecular Probes A1122) and 25  $\mu$ l of protein G beads (Amersham Biosciences 17-0618-01). Immune complexes were washed three times with CSK buffer.

Protein G beads were resuspended in an equal volume of 2 $\times$  Laemmli buffer, boiled for 5 min, and resolved by SDS-PAGE. Twenty percent of each input

fraction was also analyzed by SDS-PAGE. After transfer to nitrocellulose, immunoblotting was performed with GFP antibody (Molecular Probes A11122) at 2  $\mu$ g/ml and HA-antibody (Santa Cruz sc-805) at 0.2  $\mu$ g/ml.

**Reproducibility.** All data shown are representative of experiments that were repeated at least three times with similar results on each separate occasion.

## RESULTS

**PCNA is monoubiquitinated in response to BPDE.** We previously showed that ectopically expressed GFP-Pol $\kappa$  redistributes and colocalizes with replication forks in BPDE-treated cells (6). The Lehman and Yamaizumi laboratories reported that PCNA undergoes monoubiquitination and recruits the TLS enzyme Pol $\eta$  to stalled forks in genotoxin-treated cells (28, 43). In contrast to Pol $\eta$ , mechanisms of Pol $\kappa$  regulation are not well understood. Therefore, we asked if similar PCNA-dependent mechanisms recruit Pol $\kappa$  and Pol $\eta$  to stalled replication forks.

First, we determined whether BPDE treatment induced PCNA monoubiquitination concomitant with the S-phase checkpoint. H1299 cells were chosen for these experiments. We and others have studied DNA replication extensively in this cell line (6, 20, 42). Importantly, we have demonstrated that the BPDE-induced S-phase checkpoint is intact and that GFP-Pol $\kappa$  is recruited to sites of ongoing DNA replication in H1299 cells. H1299 cells were treated with 100 or 600 nM BPDE. At different times after BPDE treatment, nuclear fractions were prepared from BPDE-treated cells and assayed for monoubiquitinated PCNA, which is detected as a distinct band of  $\sim$ 40 kDa, in contrast to unmodified PCNA, which is  $\sim$ 32 kDa on immunoblots.

The inhibition of DNA synthesis induced by 100 nM BPDE results mainly from inhibition of initiation of replication unfired origins (12, 29). In a previous report, we have shown that 100 nM BPDE elicits a transient inhibition of DNA synthesis that is maximal 1 to 3 h after BPDE treatment (20). As shown in Fig. 1A, 100 nM BPDE induced a modest (1.6-fold) increase in the levels of an anti-PCNA immunoreactive band of 40 kDa, which corresponds to the correct size for monoubiquitinated PCNA. The amount of putative monoubiquitinated PCNA declined to basal levels by 3 to 5 h after BPDE treatment, concomitant with recovery from the S-phase checkpoint. Therefore, the kinetics of PCNA modification induced by 100 nM BPDE were similar to the kinetics of inhibition of DNA synthesis. In contrast to the transient inhibition of DNA synthesis elicited by 100 nM BPDE, 600 nM BPDE results in a persistent inhibition of DNA synthesis due to inhibition of both initiation and elongation steps of DNA synthesis (12, 29). Inhibition of elongation represents a physical stalling of replication forks and is not a regulated checkpoint response. PCNA was also posttranslationally modified in a manner consistent with its monoubiquitination in cells treated with 600 nM BPDE, concomitant with inhibition of elongation. However, both the duration and the levels of PCNA modification were increased in cells treated with the higher dose of BPDE (Fig. 1A, bottom).

Based on the apparent molecular weight of the posttranslationally modified PCNA induced by BPDE, and because of previous studies showing that PCNA is monoubiquitinated in response to DNA damage, it appeared likely that BPDE induced a monoubiquitinated form of PCNA. However, PCNA may be subject to other posttranslational modifications that affect its mobility (22). Therefore, we performed experiments

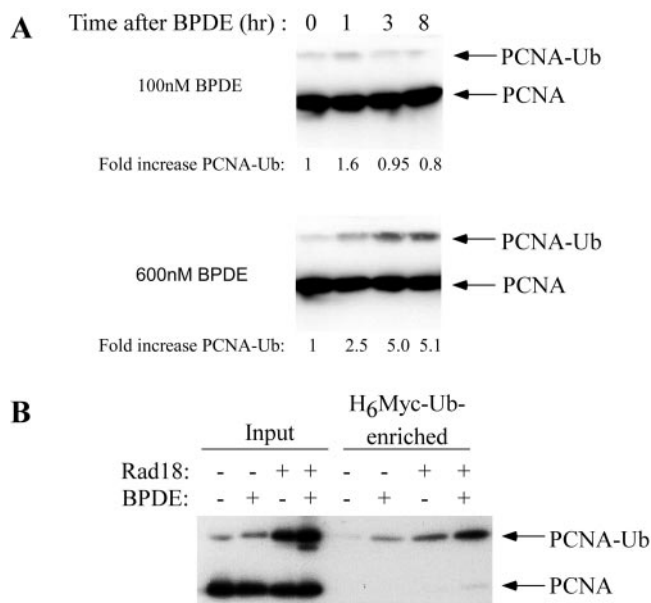


**FIG. 1.** PCNA is monoubiquitinated after BPDE treatment. (A) Exponentially growing H1299 cells were treated with 100 nM (top) or 600 nM (bottom) BPDE. At different time points after BPDE treatment, nuclear fractions were prepared. After normalizing for protein content, nuclear samples were separated by SDS-PAGE, transferred to nitrocellulose, and analyzed by immunoblotting with anti-PCNA antibodies. (B) H1299 cells were infected with AdCon or AdRad18 for 24 h. The resulting cultures were transfected with H<sub>6</sub>M-Ub for 24 h and treated with BPDE (or left untreated). After 4 h, chromatin fractions from the cells were analyzed directly for PCNA levels. Alternatively, H<sub>6</sub>M-Ub-conjugated proteins were purified with cobalt-agarose resin prior to immunoblot analysis with anti-PCNA.

to test specifically if PCNA is ubiquitinated after BPDE treatment.

We expressed a hexahistidine- and Myc-tagged form of Ub (designated H<sub>6</sub>M-Ub) in AdCon (empty adenovirus vector)- or AdRad18 (encoding Rad18, a PCNA E3 ligase)-infected H1299 cells by transient transfection. The resulting H<sub>6</sub>M-Ub-expressing cells were given BPDE or left untreated as controls. H<sub>6</sub>M-Ub-containing proteins were purified from chromatin fractions with metal affinity resin as described in Materials and Methods. The resulting H<sub>6</sub>M-Ub-conjugated proteins were resolved by SDS-PAGE and probed with an anti-PCNA antibody. As shown in Fig. 1B, both BPDE and Rad18 induced a 45-kDa PCNA species that was enriched by metal affinity purification. Forty-five kilodaltons corresponds to the expected molecular mass of H<sub>6</sub>M-Ub-tagged and monoubiquitinated PCNA. This result demonstrates that PCNA is ubiquitinated in response to BPDE treatment and Rad18 overexpression.

Taken together, these results show that PCNA is ubiquitinated concomitant with the BPDE-induced inhibition of DNA synthesis caused by BPDE doses that inhibit late origin firing (100 nM BPDE) or concentrations that elicit blocks in elongation (600 nM BPDE). The temporal pattern of BPDE-induced PCNA ubiquitination shown here correlates well with the pattern of GFP-Pol $\kappa$  focus formation that we described in a previous study (6). These data are consistent with a putative role for PCNA ubiquitination in Pol $\kappa$  regulation.

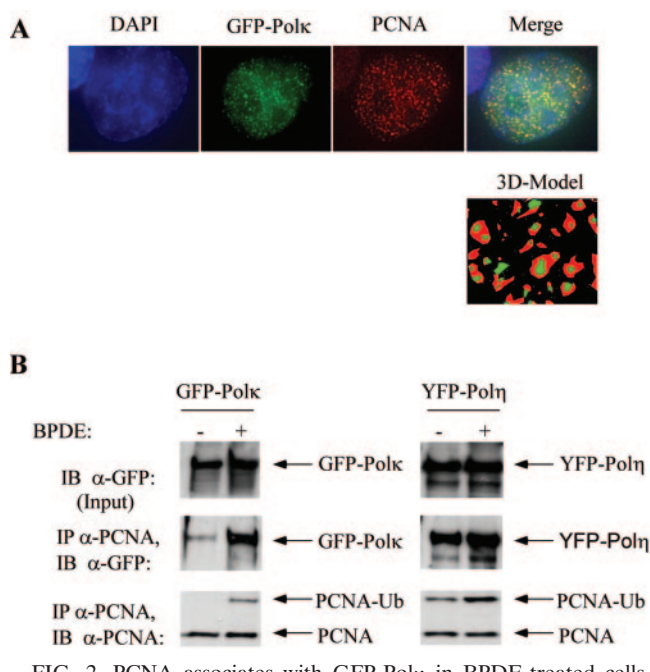


FIG. 2. PCNA associates with GFP-Pol $\kappa$  in BPDE-treated cells. (A) H1299 cells growing in chamber slides were infected with AdGFP-Pol $\kappa$  for 24 h. The resulting cultures were treated with BPDE, and 6 h later cells were fixed with formaldehyde. The resulting slides were probed with anti-PCNA. Bound PCNA antibody was detected with Cy3-coupled secondary antisera. PCNA and GFP-Pol $\kappa$  fluorescence were visualized by DeltaVision deconvolution microscopy. DeltaVision 3D object-builder software was used to generate a three-dimensional model of the two-dimensional polygons in each z section of a representative quadrant within the nucleus. The schematic depicts the degree to which green (GFP-Pol $\kappa$ ) and red (PCNA) signals colocalize in three dimensions. (B) H1299 cells expressing GFP-Pol $\kappa$  (left side) or YFP-Pol $\eta$  (right side) were treated with 600 nM BPDE. After 6 h, chromatin fractions from the cells were analyzed directly for Pol $\kappa$  or Pol $\eta$  levels (upper blots). Alternatively, chromatin fractions were immunoprecipitated with anti-PCNA antibodies and the resulting immunoprecipitates were analyzed for PCNA and associated GFP-Pol $\kappa$  or YFP-Pol $\eta$  with anti-GFP antibodies. IB, immunoblotting.

**GFP-Pol $\kappa$  associates with PCNA in BPDE-treated cells.** Our previous study demonstrated colocalization of GFP-Pol $\kappa$  with replication forks (as identified by bromodeoxyuridine-labeled regions) in BPDE-treated cells (6). To test specifically if Pol $\kappa$  colocalizes with PCNA, we treated GFP-Pol $\kappa$ -expressing H1299 cells with BPDE, fixed the resulting cells, and probed them with anti-PCNA antibodies. We detected bound anti-PCNA antisera with Cy3-coupled secondary antibodies. Patterns of PCNA and GFP fluorescence were visualized by deconvolution microscopy. A representative nucleus showing the distribution of BPDE-induced GFP-Pol $\kappa$  foci (green) and PCNA (red) staining is shown in Fig. 2A. As shown in Fig. 2A, there was extensive (although not complete) overlap between GFP and PCNA fluorescence, indicating colocalization of Pol $\kappa$  and PCNA.

We performed co-IP experiments to determine if Pol $\kappa$  was present in a complex with PCNA after BPDE treatment. For comparison, we also performed parallel assays to measure association of Pol $\eta$  with PCNA under the same experimental conditions. H1299 cells were infected with adenovirus encod-

ing GFP-Pol $\kappa$ , YFP-Pol $\eta$ , or GFP as controls. The resulting cells were treated with 600 nM BPDE for 6 h (or left untreated) and then lysed to prepare chromatin extracts. The resulting chromatin extracts were analyzed directly for PCNA and Pol $\kappa$  or Pol $\eta$  expression by immunoblotting or solubilized and immunoprecipitated with PCNA antibodies prior to blotting with PCNA or GFP antibodies.

As shown in Fig. 2B, BPDE treatment had no effect on the levels of GFP-Pol $\kappa$ , YFP-Pol $\eta$ , or PCNA in chromatin extracts. However, as expected, PCNA ubiquitination was induced by BPDE. Anti-PCNA immunoprecipitates from the chromatin fractions were resolved by SDS-PAGE and then immunoblotted with anti-GFP (to detect coimmunoprecipitated YFP-Pol $\eta$  and GFP-Pol $\kappa$ ) or anti-PCNA (to confirm IP of PCNA).

As shown in Fig. 2B, the amount of GFP-Pol $\kappa$  that coimmunoprecipitated with PCNA was increased approximately sixfold by BPDE treatment. Interestingly, although YFP-Pol $\eta$  and GFP-Pol $\kappa$  were expressed at similar levels, there was a relatively high basal level of association between Pol $\eta$  and PCNA (the association between Pol $\eta$  and PCNA was also increased by BPDE treatment). In our previous study, we noted that YFP-Pol $\eta$ , but not GFP-Pol $\kappa$ , forms large numbers of foci in H1299 cells in the absence of genotoxin treatment (6). Therefore, Pol $\kappa$  shows a DNA damage-induced association with PCNA concomitant with its redistribution to nuclear foci. In contrast, Pol $\eta$  is associated with PCNA and subnuclear foci in H1299 cells that do not receive genotoxin. In these experiments, we noticed that overexpression of YFP-Pol $\eta$  (but not of GFP-Pol $\kappa$ ) resulted in increased monoubiquitination of PCNA, even in the absence of DNA damage (Fig. 2B, PCNA immunoblot, right side). YFP-Pol $\eta$ -induced PCNA ubiquitination likely accounts for the high basal association of PCNA with YFP-Pol $\eta$  in H1299 cells.

Previously it was shown that Pol $\eta$  is required for genotoxin-induced association of Pol $\kappa$  with nuclear foci (27). To test if Pol $\eta$  is similarly required to recruit Pol $\kappa$  to PCNA, XPV cells (which lack functional Pol $\eta$ ) were infected with adenovirus encoding GFP-Pol $\kappa$ . The resulting cells were treated with 600 nM BPDE for 4 h (or left untreated) and then lysed to prepare chromatin extracts. The resulting chromatin extracts were analyzed directly for PCNA and Pol $\kappa$  expression by immunoblotting or solubilized and immunoprecipitated with PCNA antibodies prior to blotting with PCNA or GFP antibodies.

As shown in Fig. 3A, BPDE treatment had no effect on the levels of chromatin-associated GFP-Pol $\kappa$  in XPV cells. We consistently observed an increase in levels of chromatin-bound PCNA in XPV cells after BPDE treatment. Nevertheless, as expected, BPDE induced PCNA ubiquitination in XPV cells. Moreover, as also shown in Fig. 3A, BPDE induced association of GFP-Pol $\kappa$  with PCNA, similar to results of experiments with Pol $\eta$ -expressing H1299 cells (Fig. 2). Therefore, Pol $\kappa$  recruitment to PCNA is BPDE inducible in the absence of Pol $\eta$ .

To further investigate if Pol $\kappa$  and Pol $\eta$  are regulated coordinately in response to DNA damage, we investigated the relative subcellular distribution of these polymerases in control and BPDE-treated cells. H1299 cells were cotransfected with HA-Pol $\kappa$  and YFP-Pol $\eta$  expression plasmids. Two days after transfection, cells were treated with 600 nM BPDE for 6 h and then solubilized with CSK buffer to remove soluble proteins.

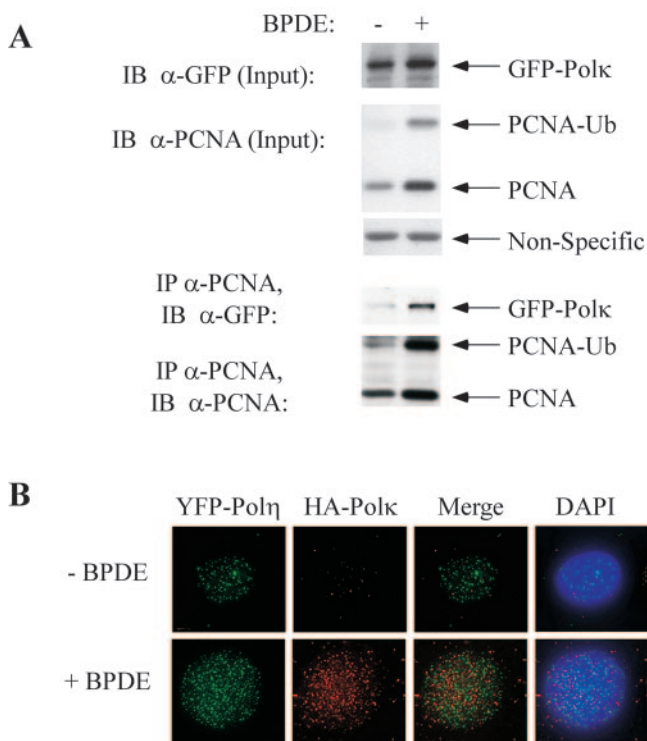


**FIG. 3.** Pol $\eta$  is not required for BPDE-induced association of Polk with PCNA. (A) CRL1162-TERT XPV cells were infected with  $2 \times 10^{10}$  PFU/ml of AdGFP-Pol $\kappa$ . At 48 h after infection, cells were given 600 nM BPDE or left untreated as controls. After 4 h, chromatin fractions were prepared and analyzed directly for Polk and PCNA levels (top). Alternatively, chromatin fractions were immunoprecipitated with anti-PCNA antibody. The resulting immunoprecipitates were resolved by SDS-PAGE, transferred to nitrocellulose, and probed with anti-GFP or anti-PCNA antibodies (bottom). (B) H1299 cells were cotransfected with expression plasmids for YFP-Pol $\eta$  and HA-Pol $\kappa$ . At 48 h after transfection, cells were treated with 600 nM BPDE for 6 h. Cells were washed with CSK buffer to remove soluble proteins. The resulting nuclei were fixed in formaldehyde and immunostained with anti-HA antibody. Slides were visualized by Delta-Vision deconvolution microscopy. IB, immunoblotting.

Then chromatin-associated HA-Pol $\kappa$  and YFP-Pol $\eta$  were visualized by fluorescence microscopy.

As shown in Fig. 3B, and consistent with our previous report (6), YFP-Pol $\eta$  formed nuclear foci in the absence of BPDE. However, there was an increase in the number of YFP-Pol $\eta$  foci in each cell after BPDE treatment. In contrast, HA-Pol $\kappa$  foci were observed only after BPDE treatment (Fig. 3B). We observed remarkably little colocalization of HA-Pol $\kappa$  and YFP-Pol $\eta$  foci in BPDE-treated cells. These data are consistent with the results of Fig. 3A, which demonstrate that Pol $\eta$  is not required for BPDE-induced recruitment of Polk to replication forks.

Since the experiments whose results are shown in Fig. 1 demonstrated BPDE-induced PCNA ubiquitination and BPDE-induced association between PCNA and GFP-Pol $\kappa$ , we asked if this association required PCNA ubiquitination. We generated adenovirus vectors that express HA-tagged WT PCNA and HA-tagged PCNA K164A encoding a ubiquitination-resistant mutant form of PCNA. To verify that the K164A mutant was not ubiquitinated, we expressed HA-PCNA-WT and HA-PCNA-K164A in H1299

cells by adenoviral infection. The resulting cultures were treated with 600 nM BPDE or coinfecting with AdRad18. Chromatin extracts were prepared, resolved by SDS-PAGE, transferred to nitrocellulose, and then probed with HA antibodies. As expected, HA-PCNA-WT but not HA-PCNA-K164A underwent a monoubiquitination-induced mobility shift in response to BPDE treatment or Rad18 overexpression (Fig. 4A).

H1299 cells were coinfecting with adenoviral vectors encoding GFP-Pol $\kappa$  and WT or K164A PCNA. The resulting cultures were treated with BPDE and lysed to prepare nuclear fractions. Solubilized chromatin extracts were immunoprecipitated with anti-HA antisera to recover ectopically expressed WT or mutant PCNA. The resulting immune complexes were separated by SDS-PAGE, blotted, and then probed with anti-GFP antisera to detect GFP-Pol $\kappa$ . Similar to the experiment in Fig. 2, in which we detected association between GFP-Pol $\kappa$  and endogenous PCNA, HA-tagged WT PCNA associated with GFP-Pol $\kappa$  in a BPDE-inducible fashion (Fig. 4B). In contrast, in the parallel experiment performed with HA-tagged K164A PCNA, we detected no basal or DNA damage-induced co-IP of GFP-Pol $\kappa$ . Taken together, our results indicate that BPDE-induced association between Polk and PCNA requires ubiquitination on K164 of PCNA. This is similar to the mechanism proposed for recruitment of Pol $\eta$  to PCNA (28). However, as shown in our experiments in Fig. 2B, there are clear differences in the levels of PCNA-associated Polk and Pol $\eta$  without BPDE treatment which are proportional to the level of monoubiquitinated PCNA.

**Rad18 status influences association between PCNA and Polk.** The results shown in Fig. 1 to 3 suggested a role for PCNA monoubiquitination in Polk regulation. Studies with yeast and mammalian cells have shown that PCNA monoubiquitination in response to genotoxins requires the E3 ligase Rad18 (22, 28, 39, 43). Therefore, we used siRNA strategies to test the role of Rad18 in BPDE-induced PCNA ubiquitination and Polk regulation.

We tested the effectiveness of Rad18 siRNA on levels of ectopically expressed HA-tagged Rad18 protein. H1299 cells were infected with Ad-HARad18 adenovirus. The resulting cultures were transfected with siRNA against Rad18 or control Cy3 RNA oligonucleotides. Protein extracts from these cultures were separated by SDS-PAGE, blotted to nitrocellulose, and then probed with anti-HA antibodies. As shown in Fig. 4C, HA-Rad18 was readily detected in extracts from cells transfected with control RNA oligonucleotides. However, expression of HA-Rad18 was ablated by >90% in Rad18 siRNA-transfected cells. Therefore, our Rad18 siRNA oligonucleotides were effective for silencing Rad18 expression.

We tested the effects of Rad18 siRNA on BPDE-induced monoubiquitination of PCNA and PCNA-Pol $\kappa$  interactions. H1299 cells were infected with AdGFP-Pol $\kappa$  and then transfected with control or Rad18 siRNA oligonucleotides. The resulting cells were treated with BPDE or left untreated as controls. After lysis, chromatin extracts from the cells were immunoprecipitated with anti-PCNA antibodies and analyzed for PCNA modification and coimmunoprecipitated GFP-Pol $\kappa$ .

As shown in Fig. 4D, BPDE induced PCNA monoubiquitination and association between PCNA and GFP-Pol $\kappa$  in Cy3-transfected (control) cells. However, both the BPDE-induced increase in monoubiquitinated PCNA and PCNA-bound GFP-

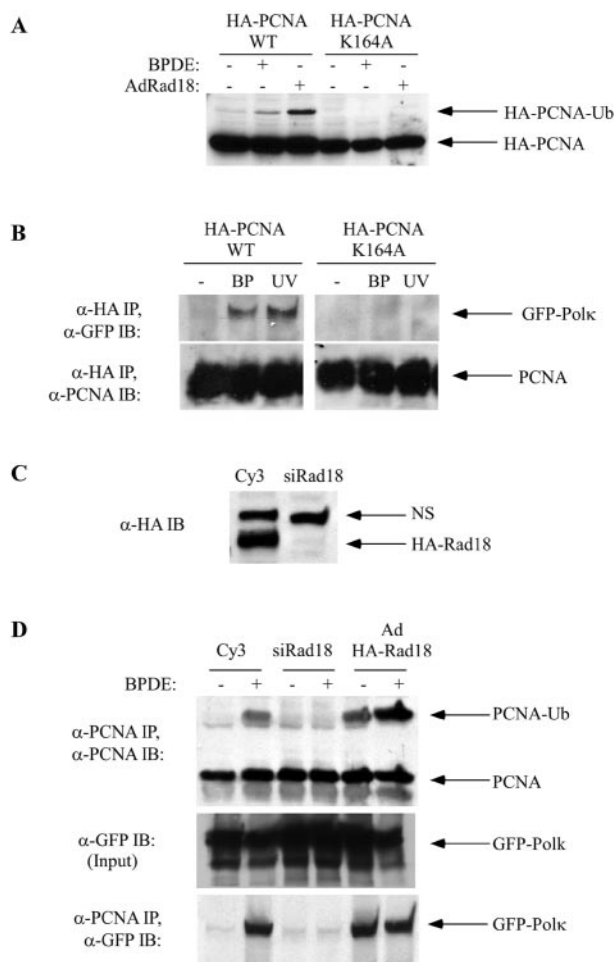


FIG. 4. DNA damage-induced association between GFP-Polκ and PCNA requires Rad18-dependent PCNA monoubiquitination. (A) H1299 cells were infected with AdHA-PCNA-WT or AdHA-PCNA-K164A individually or in combination with AdHA-Rad18. At 48 h postinfection, some cultures were treated with 600 nM BPDE. Cells were harvested 6 h after BPDE treatment. Chromatin fractions were collected and analyzed for expression of HA-tagged PCNA. (B) H1299 cells were coinfecting with AdGFP-Polκ and AdHA-PCNA-WT or AdHA-PCNA-K164A. Twenty-four hours after infection, cells were given 600 nM BPDE (BP) or 10 J/m<sup>2</sup> of UVC (UV) or left untreated as controls. At 6 h after genotoxin treatment, chromatin fractions were prepared and immunoprecipitated with anti-HA antibody. The resulting immunoprecipitates were resolved by SDS-PAGE, transferred to nitrocellulose, and probed with anti-GFP (top) or anti-PCNA (bottom) antibodies. (C) H1299 cells were infected with AdHA-Rad18 for 24 h. The HA-Rad18-expressing cells were transfected with siRNA oligonucleotides against Rad18 (siRad18) or with control (Cy3) oligonucleotides. The resulting cells were lysed 24 h later. Cell extracts were resolved by SDS-PAGE, transferred to nitrocellulose, and analyzed by blotting with anti-HA antibodies. NS indicates a protein present in H1299 cell lysates that reacts nonspecifically with polyclonal anti-HA antisera and serves as a loading control. (D) H1299 cells were transfected with siRNA oligonucleotides against Rad18 (siRad18) or control siRNA oligonucleotides (Cy3) or infected with AdHA-Rad18. Twenty-four hours later, cells were given 600 nM BPDE for 6 h or left untreated as controls. Chromatin extracts from the cells were immunoprecipitated with anti-PCNA antisera. Immunoprecipitates were analyzed by Western blotting with antibodies against PCNA or GFP. IB, immunoblotting.

Polκ were ablated in Rad18 siRNA-transfected cells. These data suggest that Rad18 is required for BPDE-induced associations between Polκ and PCNA.

We also determined the effect of Rad18 overexpression on PCNA ubiquitination and PCNA-Polκ interactions. Adenovirus vectors were used to express GFP-Polκ individually or in combination with HA-tagged Rad18. Rad18-overexpressing cells had very high basal levels of monoubiquitinated PCNA, equivalent to levels of monoubiquitination induced by BPDE under our standard experimental conditions (Fig. 4D). The high basal levels of PCNA ubiquitination in AdRad18-infected cells were further increased after BPDE treatment. Interestingly, in HA-Rad18-expressing cells there was also a high-level association between PCNA and GFP-Polκ. Therefore, overexpressed Rad18 induces PCNA ubiquitination and associations between PCNA and GFP-Polκ in the absence of DNA damage. These results demonstrate an important role for Rad18 in Polκ regulation.

**Interactions between Rad18 and Polκ.** Recently, Watanabe et al. showed that Rad18 directly interacts with Polη and that the interaction is required for Polη to form nuclear foci after DNA damage (43). We performed reciprocal co-IP experiments to investigate if similar associations exist between Rad18 and Polκ. As a positive control for these experiments, we measured association between Rad18 and Polη. Chromatin fractions from cells expressing HA-Rad18 and YFP-Polη or GFP-Polκ were fixed and sheared by sonication as described by Watanabe et al. (43). Solubilized chromatin fractions were immunoprecipitated with anti-GFP antisera, and the resulting immune complexes were analyzed for associated HA-Rad18 by SDS-PAGE and Western blotting.

As expected, Rad18 was present in anti-GFP immunoprecipitates from YFP-Polη-expressing cells (Fig. 5A, lower right part). Interestingly, anti-GFP immunoprecipitates from GFP-Polκ- and YFP-Polη-expressing cells contained similar amounts of Rad18, indicating that the two polymerases associated with Rad18 to similar extents. It should be noted, however, that only a small fraction of the cellular HA-Rad18 associated with Polκ and Polη in these experiments. Moreover, the association between Polκ (or Polη) and Rad18 was only evident in immunoprecipitated chromatin fractions derived from formaldehyde-fixed nuclei. Even when we massively overexpressed GFP-Polκ or YFP-Polη and HA-Rad18, we were unable to detect association between soluble pools of polymerase and Rad18 or associations between unfixed chromatin-bound proteins (L.R.B. and C.V., data not shown). Therefore, it is likely that the associations between TLS polymerases and Rad18 that we detected in our chromatin IP assays are indirect and perhaps mediated by PCNA and/or DNA. Alternatively, putative direct associations that exist between Polκ or Polη and Rad18 might be weak, transient, and dynamic or poorly preserved *in vitro* under the experimental conditions used in this study.

Therefore, in an alternative strategy to investigate links between Rad18 and Polκ in intact cells, we determined the effect of Rad18 expression on the subcellular distribution of GFP-Polκ. H1299 cells were infected with a combination of AdGFP-Polκ and AdHA-Rad18. Twenty-four hours postinfection, the cells were treated with BPDE (or left untreated as controls) and then fixed and stained with Cy3-coupled anti-HA antibodies to detect ectopically expressed Rad18. We used decon-

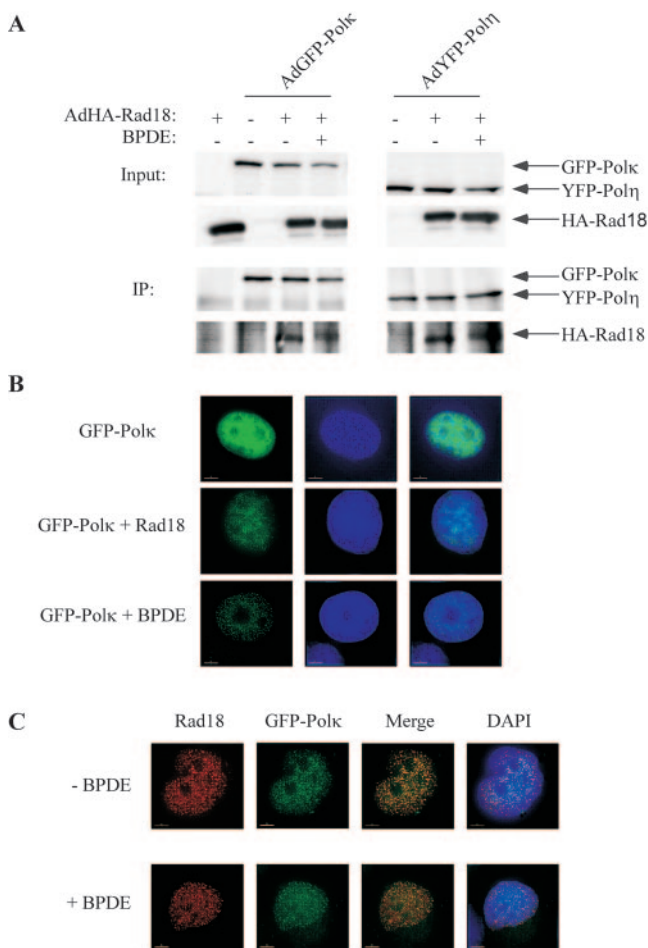


FIG. 5. Association between Rad18 and Polk. (A) H1299 cells were infected with AdGFP-Pol $\kappa$  or AdYFP-Pol $\eta$  individually or in combination with AdHA-Rad18. After 24 h, some cultures were treated with BPDE. Chromatin fractions from the resulting cells were solubilized. Aliquots of total chromatin fractions were analyzed directly for expression of HA-Rad18, GFP-Pol $\kappa$ , and YFP-Pol $\eta$  by SDS-PAGE and immunoblotting (input). The remainder of each chromatin fraction was immunoprecipitated with anti-GFP antibodies. The anti-GFP immune complexes were resolved by SDS-PAGE and probed with anti-GFP (to verify IP of GFP and YFP TLS polymerase fusion proteins) or with anti-HA (to test for associated Rad18). (B) H1299 cells were infected with AdGFP-Pol $\kappa$  individually or in combination with AdHA-Rad18. At 24 h later, some cultures were given 600 nM BPDE for 6 h. The distribution of GFP-Pol $\kappa$  in the resulting cells was determined by deconvolution microscopy. (C) H1299 cells were infected with AdGFP-Pol $\kappa$  and AdHA-Rad18. After 24 h, some cultures received 600 nM BPDE for 6 h. The resulting cells were fixed and stained with anti-HA antibodies as described in Materials and Methods.

volution immunofluorescence microscopy to determine the subcellular distribution of GFP-Pol $\kappa$  and HA-Rad18. Interestingly, when GFP-Pol $\kappa$  and HA-Rad18 were coexpressed, GFP-Pol $\kappa$  was redistributed to nuclear foci, even in the absence of BPDE treatment (Fig. 5B). The constitutive Polk nuclear foci in Rad18-expressing cells (Fig. 5C) likely result from the BPDE-independent PCNA monoubiquitination induced by ectopically expressed Rad18 (Fig. 4A and D). Nevertheless, ectopically expressed GFP-Pol $\kappa$  and HA-Rad18 colocalized in nuclear foci (Fig. 5C), consistent with the possibility that

Rad18 and Polk interact (directly or indirectly) within intact cells. These data are consistent with a role for Rad18 in Polk-mediated TLS.

**Rad18 deficiency perturbs recovery from BPDE-induced S-phase checkpoint.** The experiments described above suggested an important role for Rad18 in PCNA modification and Polk recruitment after BPDE treatment. Previously, we reported that Polk deficiency results in defective recovery from the BPDE-induced S-phase checkpoint. Since Rad18 is important for Polk regulation, we expected that *Rad18*<sup>-/-</sup> and *Polk*<sup>-/-</sup> cells would have similar checkpoint recovery defects. To test this prediction, *Rad18*<sup>-/-</sup> and WT MEFs (derived from *Rad18* knockout mice and WT animals, respectively) were analyzed for S-phase checkpoint responses to BPDE. Exponentially growing cultures of *Rad18*<sup>+/+</sup> and *Rad18*<sup>-/-</sup> cells were treated with 100 nM BPDE. Then, at different time points after BPDE treatment, we determined rates of DNA synthesis by using [<sup>3</sup>H]thymidine incorporation assays.

As shown in Fig. 6A, 2 h after BPDE treatment, DNA synthesis was reduced by 40% in *Rad18*<sup>+/+</sup> cells. However, 4 h post-BPDE treatment, rates of DNA synthesis recovered to control levels. In *Rad18*<sup>-/-</sup> cells, BPDE inhibited DNA synthesis with kinetics similar to those of WT MEFs, but DNA synthesis failed to recover to control levels within the time frame of this experiment. These data suggest a requirement for Rad18 in recovery from the BPDE-induced S-phase checkpoint. We performed similar experiments to determine the role of Rad18 in recovery from the UV-induced checkpoint. As shown in Fig. 6B, recovery from UV-induced S-phase arrest was also defective in *Rad18*<sup>-/-</sup> cells.

We considered the possibility that *Rad18*<sup>-/-</sup> cells might have a general defect in recovery from S-phase arrest. Therefore, we examined recovery from S-phase arrest induced by other agents, including IR (which induces DNA DSBs) and HU (which depletes deoxynucleoside triphosphate pools required for DNA synthesis). Figure 6C and D show the rates of DNA synthesis in *Rad18*<sup>+/+</sup> and *Rad18*<sup>-/-</sup> cells at different times after treatment with IR and HU, respectively. As shown in these experiments, the kinetics of inhibition of DNA synthesis after HU or IR treatment, and the kinetics with which DNA synthesis resumed, were indistinguishable between *Rad18*<sup>+/+</sup> and *Rad18*<sup>-/-</sup> cells. Therefore, the defective recovery of *Rad18*<sup>-/-</sup> cells from the S-phase checkpoint is relatively specific for BPDE- and UV-induced lesions. We have observed no loss of viability (as measured by trypan blue staining) in BPDE-treated or UV-irradiated *Rad18*<sup>+/+</sup> or *Rad18*<sup>-/-</sup> cells during the ~8-h time period of the DNA synthesis measurements (X.B. and C.V., data not shown). Therefore, defective checkpoint recovery of *Rad18*<sup>-/-</sup> cells (as measured by our DNA synthesis assays) is not simply a consequence of increased mortality after genotoxin treatment.

It was formally possible that defects other than *Rad18* deletion resulted in the checkpoint recovery defects we observed in *Rad18*-null MEFs. To address this possibility, we performed transient-expression experiments to reconstitute Rad18 in *Rad18*<sup>-/-</sup> MEFs. As shown in Fig. 6E, ectopic expression of HA-Rad18 corrected the defective checkpoint recovery of *Rad18*<sup>-/-</sup> cells. Taken together, our data show that Rad18 is required for recovery from the BPDE-induced S-phase checkpoint.

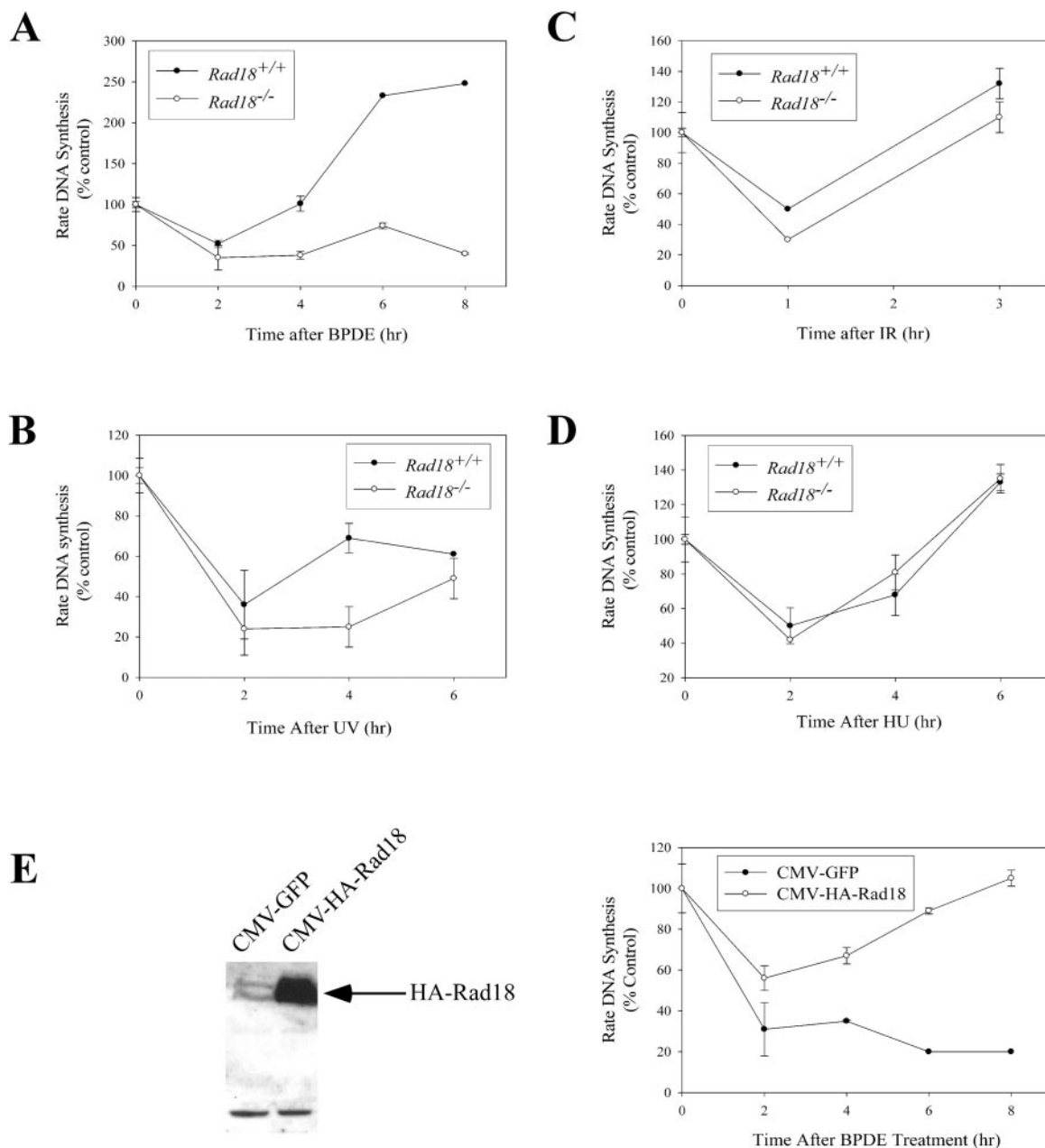


FIG. 6. S-phase checkpoint recovery defects in *Rad18*<sup>-/-</sup> MEFs. Exponentially growing cultures of *Rad18*<sup>+/+</sup> or *Rad18*<sup>-/-</sup> cells were treated with 100 nM BPDE (A), 10 J/m<sup>2</sup> UVC (B), 5 Gy of IR (C), or 2 mM HU (D). At different times after genotoxin treatments, rates of DNA synthesis of the resulting cultures were determined by [<sup>3</sup>H]thymidine incorporation assays. In the experiment shown in panel E, *Rad18*<sup>-/-</sup> MEFs were transiently transfected with cytomegalovirus (CMV)-GFP or CMV-HA-Rad18 plasmids. Transfection efficiency was >90% as determined by green fluorescence of transfected cells. Twenty-four hours after transfection, some cells were lysed and analyzed for Rad18 expression by immunoblotting with anti-HA antibodies (left side). Other cultures were treated with 100 nM BPDE. Then, at different times after BPDE treatment, rates of DNA synthesis were determined by [<sup>3</sup>H]thymidine incorporation assays.

**Checkpoint signaling in *Rad18*<sup>-/-</sup> cells.** S-phase checkpoint signaling is thought to result when replicative enzymes encounter DNA lesions, thereby uncoupling the activities of replicative helicases from fork progression (9). Our results suggested that replication forks in *Rad18*-null cells fail to carry out TLS of BPDE-adducted DNA and remain stalled. Therefore, we predicted that checkpoint signaling would be elevated in *Rad18*<sup>-/-</sup> cells relative to WT cells (which accumulate fewer

blocked replication forks). To test this prediction, we treated cultures of *Rad18*<sup>+/+</sup> or *Rad18*<sup>-/-</sup> cells with 100 nM BPDE. At different time points after BPDE treatment, the cells were lysed and the resulting protein extracts were analyzed for activation of checkpoint kinases. Chk1 is activated by replication blocks, and we previously showed that Chk1 mediates BPDE-induced S-phase arrest (20). We determined the activation status of Chk1 by using phosphospecific antisera against serine

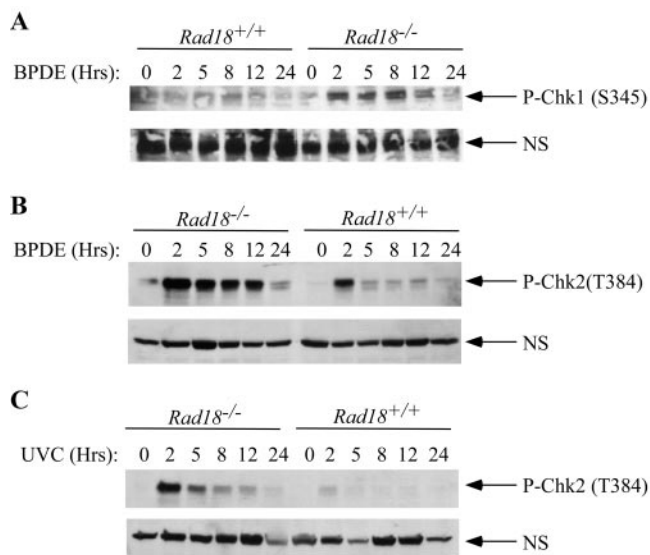


FIG. 7. Checkpoint signaling in *Rad18*<sup>-/-</sup> MEFs. *Rad18*<sup>+/+</sup> or *Rad18*<sup>-/-</sup> MEFs were treated with 100 nM BPDE (A and B) or 10 J/m<sup>2</sup> UV (C). At different times after genotoxin treatment, cells were lysed and the resulting protein extracts were analyzed for activation of checkpoint kinases with phosphospecific antibodies against Chk1 (A and B) or Chk2 (C). NS indicates nonspecific bands recognized by the antibodies that served as loading controls.

345. As shown in Fig. 7A, 100 nM BPDE elicited more persistent and higher levels of Chk1 phosphorylation in *Rad18*-deficient cells compared with WT cells. This result is consistent with the presence of persistent stalled forks resulting from BPDE treatment in a *Rad18*-null background.

Stalled replication forks are prone to breakage if left unprotected (10). If Rad18/Polk-mediated TLS contributes to protection or elimination of stalled forks, we expected that defective TLS of BPDE-adducted DNA might result in increased formation of DNA DSBs. In contrast to bulky adducts and replication blocks that principally elicit ATR/Chk1 signaling, DSBs are considered to activate ATM/Chk2 signaling pathways (3). We used the protein extracts from BPDE-treated *Rad18*<sup>+/+</sup> and *Rad18*<sup>-/-</sup> cells to monitor active Chk2 (which is readily detected with phosphospecific antisera against phospho-T384). As shown in Fig. 7B, Chk2 phosphorylation was strongly induced by BPDE treatment in *Rad18*<sup>-/-</sup> cells (but not in *Rad18*<sup>+/+</sup> cultures). We obtained similar results in experiments with UV as a genotoxin (Fig. 7C). Collectively, these results suggest that secondary forms of DNA damage (including DSBs) are generated from persistently stalled replication forks in *Rad18*-deficient cells.

We showed previously that Polk is important for cell survival after BPDE treatment (6). It was of interest to determine if Rad18 was similarly required for cell viability after acquisition of BPDE-induced DNA damage. Exponentially growing cultures of WT and *Rad18*<sup>-/-</sup> cells were given BPDE or other genotoxins for the purpose of comparison. After 24 h, control and genotoxin-treated cultures were trypsinized and replated at a density of 100 cells/10-cm dish. One week later, viable colonies were visualized by Giemsa staining and enumerated. As shown in the bar chart in Fig. 8, 40% of the *Rad18*<sup>+/+</sup>

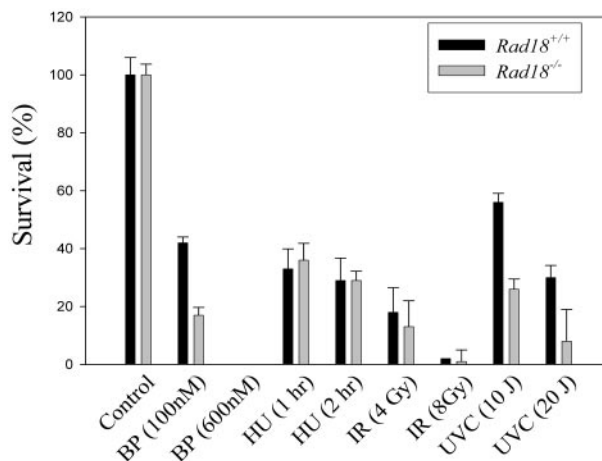


FIG. 8. Clonogenic survival of *Rad18*<sup>+/+</sup> and *Rad18*<sup>-/-</sup> cells after genotoxin treatment. Exponentially growing cultures of *Rad18*<sup>+/+</sup> or *Rad18*<sup>-/-</sup> MEFs were treated with BPDE (BP; 100 nM or 600 nM), HU (2 mM for 1 h or 2 h), IR (4 Gy or 8 Gy), or UVC (10 J/m<sup>2</sup> or 20 J/m<sup>2</sup>). Twenty-four hours after treatment, cells were trypsinized and counted and then replated at a density of 1,000 cells/10-cm plate. The resulting plates were returned to the incubator and given fresh growth medium every 3 days. After 7 days, cells were fixed and stained with Giemsa. Giemsa-stained colonies containing >50 cells were scored.

cultures survived treatment with 100 nM BPDE. However, *Rad18*<sup>-/-</sup> cells only showed <20% viability after treatment with 100 nM BPDE. *Rad18*<sup>-/-</sup> cells also showed increased sensitivity to UV compared with WT MEFs (Fig. 8). However, *Rad18* status did not significantly affect the viability of HU- or IR-treated cultures (Fig. 8). Therefore, Rad18 is important for survival after acquisition of bulky fork-blocking DNA adducts resulting from BPDE or UV but is not required for viability after IR-induced DSBs or HU-induced replication cessation.

**Role of checkpoint signaling in PCNA ubiquitination and Polk recruitment.** In eukaryotes, cell cycle inhibition, apoptosis, DNA repair, and transcriptional responses to DNA damage are regulated via highly conserved checkpoint signaling pathways. For example, in mammalian cells, ATM and ATR act at a very early stage of DNA damage detection and signaling and mediate most responses to DNA damage. We have shown that the 9-1-1/ATR/Chk1 pathway is necessary for the BPDE-induced S-phase checkpoint (but that the Nbs1/ATM/Chk2 pathway is dispensable for this response). We hypothesized that 9-1-1/ATR/Chk1 checkpoint signaling might contribute to the regulation of PCNA ubiquitination and Polk recruitment to replication forks. Therefore, we have tested roles for the 9-1-1/ATR/Chk1 pathway in Polk regulation.

We previously showed that the ATM/ATR inhibitor caffeine caused a decrease in the number of Polk nuclear foci induced by BPDE treatment (6). In unpublished experiments, we also found that the Chk1 inhibitor UCN-01 decreased the number of GFP-Polk foci induced by BPDE. Those studies further suggested a role for the ATR/Chk1 pathway in PCNA modification and Polk regulation. A potential complication of studies with caffeine and UCN-01 is that these inhibitors are not entirely specific and might perturb Polk regulation in an ATR- or Chk1-independent manner. Therefore, we used siRNA and

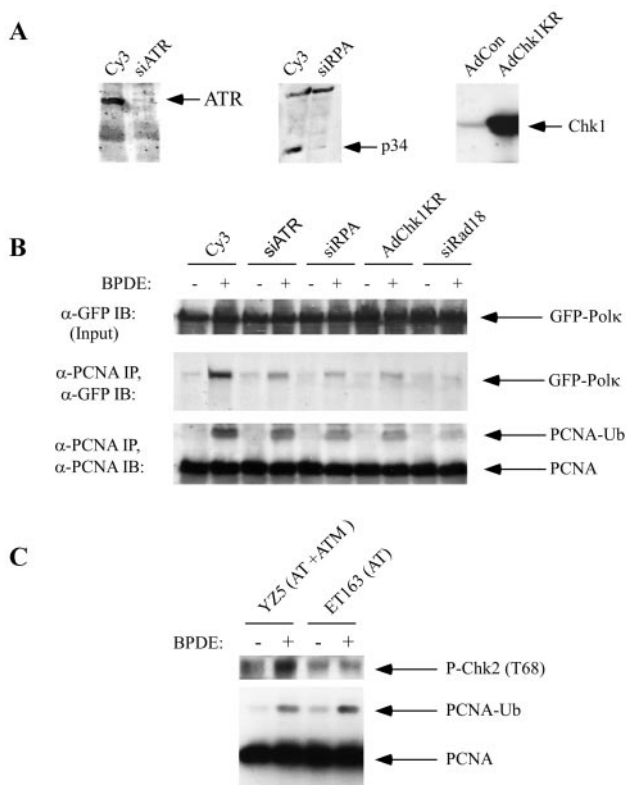


FIG. 9. Roles of RPA, ATR, and Chk1 in BPDE-induced PCNA ubiquitination and Polk recruitment. (A) H1299 cells were transfected with siRNA oligonucleotide duplexes against ATR and RPA or with control Cy3 RNA oligonucleotides. Some cultures were infected with AdChk1KR or AdCon. The resulting cells were analyzed for ATR, RPA, or Chk1 expression with appropriate antibodies. (B) H1299 cells expressing GFP-Polk were transfected with siRNA oligonucleotides against ATR, RPA, and Rad18 or with Cy3 (control) oligonucleotides. Alternatively, some cultures were infected with AdChk1KR. The resulting cultures were given 600 nM BPDE, and 6 h later the cells were lysed. Nuclear fractions were immunoprecipitated with anti-PCNA, and the resulting immune complexes were resolved by SDS-PAGE and immunoblotted (IB) with anti-PCNA or anti-GFP antibodies. (C) ET163 and YZ5 cells were treated with 600 nM BPDE or left untreated as controls. After 4 h, soluble and chromatin fractions were prepared and analyzed directly for PCNA (chromatin fraction) and Thr68-phosphorylated Chk2 (soluble fraction) levels.

dominant-negative strategies to provide a more specific test of the role of ATR/Chk1 signaling in Polk regulation.

To determine the role of ATR in Polk regulation, we performed siRNA experiments to ablate ATR expression. The ssDNA-binding protein RPA is important for activating ATR at stalled replication forks. Therefore, we performed complementary experiments with siRNA against the RPA p34 subunit to test the role of RPA in PCNA modification and Polk regulation. GFP-Polk-expressing H1299 cells were transfected with siRNA oligonucleotides against ATR or RPA or with Cy3 control RNAi duplexes. At 48 h after transfection, we prepared cell extracts and performed immunoblotting with RPA p34 and ATR antisera (Fig. 9A). These analyses verified that ATR and RPA levels were effectively ablated under our experimental conditions.

The siRNA duplex-transfected cells were treated with

BPDE (or left untreated as controls). PCNA was immunoprecipitated from solubilized chromatin extracts, and PCNA ubiquitination and levels of PCNA-associated GFP-Polk in the immune complexes were determined by immunoblotting (Fig. 9B). As expected, BPDE induced PCNA ubiquitination and association between Polk and PCNA in Cy3 control siRNA-transfected cultures. However, in cells transfected with siATR and siRPA duplexes, both PCNA ubiquitination and association between PCNA and Polk were reduced by approximately 60%.

Since Chk1 is an important effector of ATR and 9-1-1 in the S-phase checkpoint, we asked if Chk1 was involved in Polk regulation. We previously generated a kinase-inactive dominant-negative mutant form of Chk1 that we expressed with an adenovirus vector. We and others have shown that this reagent can be used to inhibit S and G<sub>2</sub> checkpoints mediated by Chk1 signaling (20, 21). Therefore, we tested the effect of dominant-negative Chk1 on the BPDE-induced association between PCNA and Polk. As shown in Fig. 9B, expression of dominant-negative Chk1 reduced the levels of monoubiquitinated PCNA and the amount of PCNA-associated Polk in BPDE-treated cells by 50% relative to those in control cultures. Therefore, Chk1 signaling contributes to PCNA modification and Polk regulation.

A recent publication by Jazayeri et al. demonstrated that ATR activation by DSBs is regulated by ATM in a cell cycle-dependent manner (24). Therefore, it was of interest to determine if ATM is required for BPDE-induced (and ATR/Chk1-dependent) PCNA ubiquitination. To test the role of ATM in BPDE-induced PCNA ubiquitination, we compared the effect of BPDE treatment on PCNA ubiquitination in ET163 fibroblasts from AT patients and in matched cells designated YZ5 that express reconstituted ATM (46). As shown in Fig. 9C, BPDE-induced PCNA ubiquitination was evident in both ET163 and YZ5 cells and therefore is ATM independent. As expected, DNA damage-induced Chk2 phosphorylation (which is known to be largely ATM dependent) was only observed in YZ5 cells. Taken together, these data suggest that efficient PCNA ubiquitination requires ATR and Chk1, but not the ATM pathway.

DISCUSSION

Our previous work demonstrated an important role for Polk in recovery from the BPDE-induced S-phase checkpoint (6). Those studies suggested that Polk is recruited to replication forks stalled by BPDE-affected DNA and that subsequent Polk-mediated lesion bypass allows attenuation of the S-phase checkpoint. Here we have investigated the mechanism(s) that recruits Polk to stalled replication forks. We show that PCNA is ubiquitinated in a Rad18-dependent manner after acquisition of DNA damage and that Polk associates specifically with monoubiquitinated PCNA. Further, consistent with a role for Rad18-mediated PCNA monoubiquitination in Polk regulation, *Rad18*<sup>-/-</sup> and *Polk*<sup>-/-</sup> cells have similar defects in recovery from the BPDE-mediated S-phase checkpoint.

Although we have shown that Polk forms a complex with monoubiquitinated PCNA, we have not demonstrated that this interaction is direct. Therefore, it is possible that the interaction of Polk with monoubiquitinated PCNA is mediated by another TLS polymerase and/or other factors. For example,

Pol $\eta$  and Pol $\iota$  interact directly and Pol $\eta$  is required for genotoxin-induced redistribution of Pol $\iota$  to replication foci (27). In contrast to Pol $\iota$ , we have shown that the recruitment of Pol $\kappa$  to ubiquitinated PCNA does not require Pol $\eta$ . Our finding that the association of Pol $\kappa$  with PCNA is Pol $\eta$  independent is consistent with previous reports that *XPV* cells do not show increased sensitivity to BPDE (8, 13) or defects in recovery from the BPDE-induced S-phase checkpoint (6).

Although Pol $\eta$  is not required for BPDE-induced association of Pol $\kappa$  with monoubiquitinated PCNA, it is possible that an alternative TLS polymerase helps recruit Pol $\kappa$  to the replication fork. However, a recent study showed that Y family polymerases, including Pol $\kappa$ , contain novel Ub-binding motifs (7), and it is also likely that Pol $\kappa$  and monoubiquitinated PCNA interact directly.

Okada et al. previously found additive effects of *Rad18* and *Polk* deletion in chicken DT40 cells (37), arguing against a dependence of Pol $\kappa$  on *Rad18* gene function in this experimental system. This contrasts with our finding that Pol $\kappa$  is regulated in a Rad18-dependent manner in mammalian cells. It is possible that Pol $\kappa$  is regulated via Rad18-independent mechanisms in avian cells. Alternatively, the Rad18 independence of Pol $\kappa$  regulation may be an idiosyncrasy of DT40 cells. Recombination activity is very high in DT40, as indicated by the very high efficiency of gene targeting in these cells. It is possible that DNA damage tolerance in DT40 depends more heavily on a DNA recombination pathway than on TLS compared with other systems. Another possibility is that the *Rad18* mutant described by Okada and colleagues is not a complete genetic null. Regardless of the reason for the Rad18 independence of Pol $\kappa$  regulation in DT40 cells, our data demonstrate a role for Rad18 in Pol $\kappa$  regulation in mammalian cell lines. As discussed above, the recent finding that Pol $\kappa$  contains a Ub-binding motif (7) provides a plausible molecular basis for direct recruitment of Pol $\kappa$  to ubiquitinated PCNA and supports a role for Rad18 in Pol $\kappa$  regulation.

Interestingly, our data indicate that ATR/Chk1-mediated S-phase checkpoint signaling may contribute to PCNA ubiquitination and Pol $\kappa$  recruitment in response to DNA damage. Taken together, our results suggest the model in Fig. 10, whereby replication blocks initiate ATR/Chk1 signaling. Chk1 activity inhibits late origin firing and stabilizes stalled replication forks. Potentially, stabilization of a stalled fork could facilitate PCNA ubiquitination and recruitment of TLS polymerases indirectly. Alternatively, Chk1 signaling could directly stimulate PCNA ubiquitination, perhaps via Rad18 activation. Subsequently, Pol $\kappa$ -mediated lesion bypass recovers the stalled replication fork, thereby attenuating checkpoint signaling and enabling resumption of DNA synthesis. In the absence of lesion bypass, stalled forks collapse to generate DSBs that elicit ATM/Chk2 signaling. A model in which ATR/Chk1 signaling is a prerequisite for TLS is not necessarily implied since overexpression of Rad18 can elicit DNA damage-independent PCNA ubiquitination. Therefore, checkpoint signaling is likely to modulate TLS but is probably not an absolute requirement for PCNA ubiquitination and Pol $\kappa$  recruitment.

Other workers have also suggested a role for checkpoint proteins in Pol $\kappa$  regulation. Kai and Wang showed that the 9-1-1 complex recruits DinB (*Schizosaccharomyces pombe* Pol $\kappa$ ) by direct interactions with Hus1p (26). In unpublished

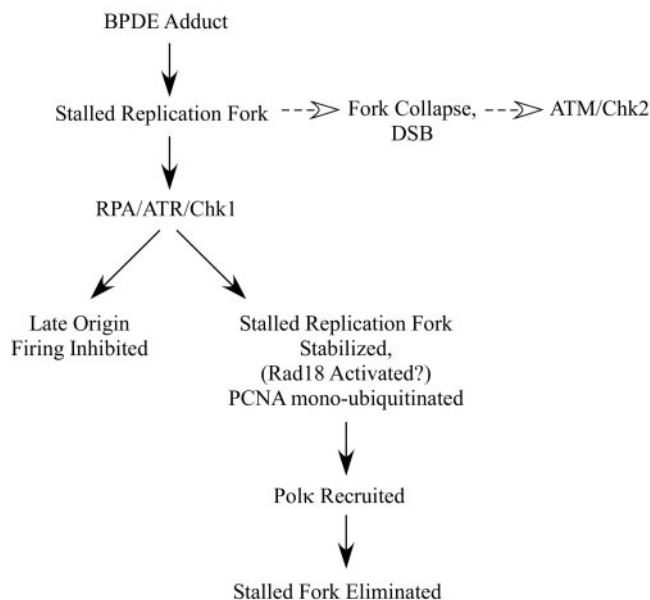


FIG. 10. Hypothetical model describing the roles of Rad18 and Pol $\kappa$  in the BPDE-induced S-phase checkpoint. Replication forks stalled by BPDE-adducted DNA activate the ATR/Chk1 pathway. ATR/Chk1 signaling inhibits firing of late origins and also stabilizes stalled replication forks. Stabilization of a stalled fork could facilitate PCNA ubiquitination and recruitment of TLS polymerases indirectly. Alternatively, Chk1 signaling could stimulate PCNA ubiquitination directly, perhaps via Rad18 activation. Pol $\kappa$  is recruited to monoubiquitinated PCNA at the stalled fork. Pol $\kappa$ -mediated lesion bypass enables recovery of the stalled replication fork, and checkpoint signaling is attenuated. In the absence of Rad18/Pol $\kappa$ , stalled forks persist and eventually collapse, generating secondary forms of damage that activate ATM/Chk2.

studies, we have also tested a putative role for 9-1-1 in Pol $\kappa$  regulation in mammalian cells. By co-IP or immunofluorescence microscopy, we were unable to demonstrate biochemical associations or colocalization between Pol $\kappa$  and 9-1-1 proteins in mammalian cells, even when using overexpressed Pol $\kappa$  and 9-1-1 components (B.X.H. and C.V., unpublished results). However, because efficient Pol $\kappa$  recruitment in mammalian cells requires Chk1 signaling, and since BPDE-induced Chk1 activation requires 9-1-1 (44), there is an indirect requirement for Hus1 in Pol $\kappa$  regulation in mammalian cells. Therefore, mammalian cells and *S. pombe* require 9-1-1 for efficient Pol $\kappa$  recruitment. The regulation of Pol $\kappa$  (and possibly other TLS enzymes) by checkpoints is likely to be conserved in eukaryotes.

We do not know the precise mechanism by which Chk1 signaling contributes to PCNA ubiquitination and Pol $\kappa$  recruitment. Checkpoint signaling could stimulate PCNA ubiquitination and interactions with TLS enzymes via phosphorylation of Rad18 and/or Pol $\kappa$ . Alternatively, the critical role of checkpoint signaling in Pol $\kappa$  recruitment might be indirect via stabilization of the stalled replication fork. The major role of the S-phase checkpoint is considered to be stabilizing the replication fork and preventing the collapse of stalled forks via an unknown mechanism(s) (16, 31, 40). Since checkpoint signaling is important for Pol $\kappa$  recruitment, it is interesting to speculate that stalled replication forks are stabilized in part via

recruitment of TLS enzymes. Clarification of these issues will require a more detailed analysis of mechanisms that stimulate PCNA ubiquitination.

The mechanism by which Rad18-mediated monoubiquitination of PCNA occurs in response to DNA damage is not clear. Potentially, PCNA ubiquitination could result from an increase in Rad18 activity, from decreased deubiquitination of PCNA, or from a combination of both mechanisms. Experimentally increasing Rad18 activity inside cells by adenovirus-mediated Rad18 overexpression is sufficient to induce PCNA modification and recruitment of Polk. Therefore, a putative mechanism based on Rad18 stimulation appears feasible and could account for the observed effects of DNA damage on PCNA ubiquitination.

Additionally, there exists a precedent for regulated deubiquitination as a branch of the DNA damage-signaling pathway. D'Andrea and colleagues showed that the deubiquitinating (DUB) enzyme USP1 is involved in removal of monoubiquitin from the FANCD2 protein and that USP1 is downregulated by proteolysis in response to DNA cross-linking agents (33). Similar to BPDE-induced PCNA modification and Polk recruitment, the ATR checkpoint kinase and RPA are required for efficient FANCD2 monoubiquitination (1). Interestingly, it was recently suggested that USP1 also removes monoubiquitin from PCNA (30). Therefore, a common USP1-dependent mechanism might be involved in activating the FA pathway and recruiting TLS enzymes to sites of damage. Alternatively, a distinct PCNA-specific DUB enzyme might be involved in regulating BPDE-induced PCNA modifications and Polk recruitment. Experiments are under way to identify putative Rad18- or DUB enzyme-dependent mechanisms that mediate the increases in monoubiquitinated PCNA after BPDE treatment.

#### ACKNOWLEDGMENTS

We thank Alain Verreault, Tim Heffernan, Bill Kaufmann, Anindya Dutta, and Yoli Sanchez for critical reading of the manuscript and for valuable comments and suggestions.

This work was supported by grants ES09558 and ES12917 from the National Institutes of Health (to C.V.) and by grants from the Japanese Ministry of Education, Culture, Sports, Science, and Technology (to S.T., M.Y., and H.O.).

#### REFERENCES

- Andreassen, P. R., A. D. D'Andrea, and T. Taniguchi. 2004. ATR couples FANCD2 monoubiquitination to the DNA-damage response. *Genes Dev.* **18**:1958–1963.
- Bailly, V., S. Lauder, S. Prakash, and L. Prakash. 1997. Yeast DNA repair proteins Rad6 and Rad18 form a heterodimer that has ubiquitin conjugating, DNA binding, and ATP hydrolytic activities. *J. Biol. Chem.* **272**:23360–23365.
- Bartek, J., C. Lukas, and J. Lukas. 2004. Checking on DNA damage in S phase. *Nat. Rev. Mol. Cell Biol.* **5**:792–804.
- Baum, E. J. 1978. Occurrence and surveillance of polycyclic aromatic hydrocarbons. Academic Press, Inc., New York, N.Y.
- Bergoglio, V., C. Bavoux, V. Verbiest, J. S. Hoffmann, and C. Cazaux. 2002. Localisation of human DNA polymerase kappa to replication foci. *J. Cell Sci.* **115**:4413–4418.
- Bi, X., D. M. Slater, H. Ohmori, and C. Vaziri. 2005. DNA polymerase kappa is specifically required for recovery from the benzo[a]pyrene-dihydrodiol epoxide (BPDE)-induced S-phase checkpoint. *J. Biol. Chem.* **280**:22343–22355.
- Bienko, M., C. M. Green, N. Crosetto, F. Rudolf, G. Zapart, B. Coull, P. Kannouche, G. Wider, M. Peter, A. R. Lehmann, K. Hofmann, and I. Dikic. 2005. Ubiquitin-binding domains in Y-family polymerases regulate translesion synthesis. *Science* **310**:1821–1824.
- Boyer, J. C., W. K. Kaufmann, B. P. Brylawski, and M. Cordeiro-Stone. 1990. Defective postreplication repair in xeroderma pigmentosum variant fibroblasts. *Cancer Res.* **50**:2593–2598.
- Byun, T. S., M. Pacek, M. C. Yee, J. C. Walter, and K. A. Cimprich. 2005. Functional uncoupling of MCM helicase and DNA polymerase activities activates the ATR-dependent checkpoint. *Genes Dev.* **19**:1040–1052.
- Cleaver, J. E., R. R. Laposa, and C. L. Limoli. 2003. DNA replication in the face of (in)surmountable odds. *Cell Cycle* **2**:310–315.
- Conney, A. H. 1982. Induction of microsomal enzymes by foreign chemicals and carcinogenesis by polycyclic aromatic hydrocarbons: G. H. A. Clowes Memorial Lecture. *Cancer Res.* **42**:4875–4917.
- Cordeiro-Stone, M. B. J., B. A. Smith, and W. K. Kaufmann. 1986. Effect of benzo[a]pyrene-diol-epoxide-I on growth of nascent DNA in synchronized human fibroblasts. *Carcinogenesis* **7**:1775–1781.
- Cordeiro-Stone, M., J. C. Boyer, B. A. Smith, and W. K. Kaufmann. 1986. Xeroderma pigmentosum variant and normal fibroblasts show the same response to the inhibition of DNA replication by benzo[a]pyrene-diol-epoxide-I. *Carcinogenesis* **7**:1783–1786.
- Costanzo, V., and J. Gautier. 2003. Single-strand DNA gaps trigger an ATR- and Cdc7-dependent checkpoint. *Cell Cycle* **2**:17.
- Costanzo, V., D. Shechter, P. J. Lupardus, K. A. Cimprich, M. Gottesman, and J. Gautier. 2003. An ATR- and Cdc7-dependent DNA damage checkpoint that inhibits initiation of DNA replication. *Mol. Cell* **11**:203–213.
- Desany, B. A., A. A. Alcasabas, J. B. Bachant, and S. J. Elledge. 1998. Recovery from DNA replicational stress is the essential function of the S-phase checkpoint pathway. *Genes Dev.* **12**:2956–2970.
- Difley, J. F. 2004. Regulation of early events in chromosome replication. *Curr. Biol.* **14**:R778–R786.
- Dipple, A. 1995. DNA adducts of chemical carcinogens. *Carcinogenesis* **16**:437–441.
- Dipple, A., Q. A. Khan, J. E. Page, I. Ponten, and J. Szeliga. 1999. DNA reactions, mutagenic action and stealth properties of polycyclic aromatic hydrocarbon carcinogens (review). *Int. J. Oncol.* **14**:103–111.
- Guo, N., D. V. Faller, and C. Vaziri. 2002. Carcinogen-induced S-phase arrest is Chk1 mediated and caffeine sensitive. *Cell Growth Differ.* **13**:77–86.
- Heffernan, T. P., D. A. Simpson, A. R. Frank, A. N. Heinloth, R. S. Paules, M. Cordeiro-Stone, and W. K. Kaufmann. 2002. An ATR- and Chk1-dependent S checkpoint inhibits replicon initiation following UVC-induced DNA damage. *Mol. Cell. Biol.* **22**:8552–8561.
- Hoegge, C., B. Pfander, G. L. Moldovan, G. Pyrowolakis, and S. Jentsch. 2002. RAD6-dependent DNA repair is linked to modification of PCNA by ubiquitin and SUMO. *Nature* **419**:135–141.
- Izumi, M., F. Yatagai, and F. Hanaoka. 2001. Cell cycle-dependent proteolysis and phosphorylation of human Mcm10. *J. Biol. Chem.* **276**:48526–48531.
- Jazayeri, A., J. Falck, C. Lukas, J. Bartek, G. C. Smith, J. Lukas, and S. P. Jackson. 2006. ATM- and cell cycle-dependent regulation of ATR in response to DNA double-strand breaks. *Nat. Cell Biol.* **8**:37–45.
- Johnson, R. E., S. Prakash, and L. Prakash. 1999. Efficient bypass of a thymine-thymine dimer by yeast DNA polymerase, Poleta. *Science* **283**:1001–1004.
- Kai, M., and T. S. Wang. 2003. Checkpoint activation regulates mutagenic translesion synthesis. *Genes Dev.* **17**:64–76.
- Kannouche, P., A. R. Fernandez de Henestrosa, B. Coull, A. E. Vidal, C. Gray, D. Zicha, R. Woodgate, and A. R. Lehmann. 2003. Localization of DNA polymerases eta and iota to the replication machinery is tightly coordinated in human cells. *EMBO J.* **22**:1223–1233.
- Kannouche, P. L., J. Wing, and A. R. Lehmann. 2004. Interaction of human DNA polymerase eta with monoubiquitinated PCNA: a possible mechanism for the polymerase switch in response to DNA damage. *Mol. Cell* **14**:491–500.
- Kaufmann, W. K., J. C. Boyer, B. A. Smith, and M. Cordeiro-Stone. 1985. DNA repair and replication in human fibroblasts treated with (±)-*r-7,8*-dihydroxy-*t-9,10*-epoxy-7,8,9,10-tetrahydrobenzo[a]pyrene. *Biochim. Biophys. Acta* **824**:146–151.
- Kennedy, R. D., and A. D. D'Andrea. 2005. The Fanconi anemia/BRCA pathway: new faces in the crowd. *Genes Dev.* **19**:2925–2940.
- Lopes, M., C. Cotta-Ramusino, A. Pelliccioli, G. Liberi, P. Plevani, M. Muzi-Falconi, C. S. Newlon, and M. Foiani. 2001. The DNA replication checkpoint response stabilizes stalled replication forks. *Nature* **412**:557–561.
- Masutani, C., R. Kusumoto, A. Yamada, N. Dohmae, M. Yokoi, M. Yuasa, M. Araki, S. Iwai, K. Takio, and F. Hanaoka. 1999. The XPV (xeroderma pigmentosum variant) gene encodes human DNA polymerase eta. *Nature* **399**:700–704.
- Nijman, S. M., T. T. Huang, A. M. Dirac, T. R. Brummelkamp, R. M. Kerkhoven, A. D. D'Andrea, and R. Bernards. 2005. The deubiquitinating enzyme USP1 regulates the Fanconi anemia pathway. *Mol. Cell* **17**:331–339.
- Ogi, T., P. Kannouche, and A. R. Lehmann. 2005. Localisation of human Y-family DNA polymerase kappa: relationship to PCNA foci. *J. Cell Sci.* **118**:129–136.
- Ogi, T., Y. Shinkai, K. Tanaka, and H. Ohmori. 2002. Polk protects mammalian cells against the lethal and mutagenic effects of benzo[a]pyrene. *Proc. Natl. Acad. Sci. USA* **99**:15548–15553.
- Ohmori, H., E. Ohashi, and T. Ogi. 2004. Mammalian Polk: regulation of its expression and lesion substrates. *Adv. Protein Chem.* **69**:265–278.

37. Okada, T., E. Sonoda, Y. M. Yamashita, S. Koyoshi, S. Tateishi, M. Yamaizumi, M. Takata, O. Ogawa, and S. Takeda. 2002. Involvement of vertebrate polk in Rad18-independent postreplication repair of UV damage. *J. Biol. Chem.* **277**:48690–48695.
38. Sorensen, C. S., R. G. Syljuasen, J. Falck, T. Schroeder, L. Ronnstrand, K. K. Khanna, B. B. Zhou, J. Bartek, and J. Lukas. 2003. Chk1 regulates the S phase checkpoint by coupling the physiological turnover and ionizing radiation-induced accelerated proteolysis of Cdc25A. *Cancer Cell* **3**:247–258.
39. Stelter, P., and H. D. Ulrich. 2003. Control of spontaneous and damage-induced mutagenesis by SUMO and ubiquitin conjugation. *Nature* **425**:188–191.
40. Tercero, J. A., and J. F. Diffley. 2001. Regulation of DNA replication fork progression through damaged DNA by the Mec1/Rad53 checkpoint. *Nature* **412**:553–557.
41. Ulrich, H. D. 2004. How to activate a damage-tolerant polymerase: consequences of PCNA modifications by ubiquitin and SUMO. *Cell Cycle* **3**:15–18.
42. Vaziri, C., S. Saxena, Y. Jeon, C. Lee, K. Murata, Y. Machida, N. Wagle, D. S. Hwang, and A. Dutta. 2003. A p53-dependent checkpoint pathway prevents rereplication. *Mol. Cell* **11**:997–1008.
43. Watanabe, K., S. Tateishi, M. Kawasuji, T. Tsurimoto, H. Inoue, and M. Yamaizumi. 2004. Rad18 guides poleta to replication stalling sites through physical interaction and PCNA monoubiquitination. *EMBO J.* **23**:3886–3896.
44. Weiss, R. S., P. Leder, and C. Vaziri. 2003. Critical role for mouse Hus1 in an S-phase DNA damage cell cycle checkpoint. *Mol. Cell. Biol.* **23**:791–803.
45. Zhou, B. B., and S. J. Elledge. 2000. The DNA damage response: putting checkpoints in perspective. *Nature* **408**:433–439.
46. Ziv, Y., A. Bar-Shira, I. Pecker, P. Russell, T. J. Jorgensen, I. Tsarfati, and Y. Shiloh. 1997. Recombinant ATM protein complements the cellular A-T phenotype. *Oncogene* **15**:159–167.
47. Zou, L., and S. J. Elledge. 2003. Sensing DNA damage through ATRIP recognition of RPA-ssDNA complexes. *Science* **300**:1542–1548.
48. Zou, L., D. Liu, and S. J. Elledge. 2003. Replication protein A-mediated recruitment and activation of Rad17 complexes. *Proc. Natl. Acad. Sci. USA* **100**:13827–13832.